

Flow Rates and Repose Angles of Wet-Processed Granulations

J. T. CARSTENSEN* and PING CHING CHAN

Abstract □ The equation of McDougall and Evans was found not to apply to granulations. The functional relationships among volumetric powder flow rates, angles of repose, and particle size were demonstrated to exhibit maxima (rather than minima) in five common pharmaceutical granulations produced by wet processing. The angular behavior of granules (such as the experienced range of angles) is explained *via* supported stacking geometries, and the shallow maxima in the angle of repose *versus* granule diameter was derived from this model.

Keyphrases □ Granulations, wet processed—relationships among volumetric powder flow rates, angles of repose, and particle size □ Flow rates, powder—relationship to angles of repose and particle size in wet-processed granulations □ Repose angles—relationship to volumetric powder flow rates and particle size in wet-processed granulations □ Particle size—relationship to volumetric powder flow rates and angles of repose in wet-processed granulations □ Dosage forms—wet-processed granulations, relationships among volumetric powder flow rates, angles of repose, and particle size

Many publications have dealt with flow rates and repose angles (1–11). Attempts to relate these two properties failed to generate firm conclusions or equations of general validity (12, 13) for powders. Flow properties are of particular interest to the pharmaceutical researcher and technologist because of the effect of flow properties on the quality of the resulting solid dosage forms (2).

BACKGROUND

Repose angle measurements for powders have been viewed with the purpose of obtaining information on the cohesion of a powder. There is a theoretical correlation between the cohesion and the repose angle of a smooth slant heap (14), but such factors as the bulk density of the sample, *i.e.*, the extent of its consolidation prior to measurement, affect the repose angle (15, 16). Therefore, it is not possible to draw quantitative conclusions regarding the cohesion from repose angles. For materials above 100 μm , this approach is still followed since such powders cannot be tested in shear cells due to crushing during consolidation and low cohesion and tensile strength. The repose angle, α , relates to the diameter, d , of a fine powder (17) *via* the inverse relationship $\alpha = (q/d) + s$, where q and s are constants for a particular powder. For a coarse powder or granulation, experimental evidence (16) indicates that α , when measured *via* flow from a funnel, gives rise to a shallow maximum at a particular particle diameter. Hence, $\alpha = h(d)$, where h denotes "function of."

Flow rates, W , are a function of particle diameter (18), so $W = g(d)$, where g denotes "function of." This function has a maximum at a particular diameter (18). Since $W = g(d)$ and $\alpha = h(d)$, it follows that $d = h^{-1}(\alpha)$ and $W = g[h^{-1}(\alpha)]$ in the regions where $h(d)$ is a monotonically increasing or decreasing function; *i.e.*, there must be a relationship between W and α , *i.e.*, $W = f(\alpha)$, where f denotes "function of." The functionalities h and g are not universal but depend on experimental parameters such as orifice diameter.

McDougall and Evans (1) derived such a relationship on theoretical grounds:

$$W = \frac{\pi}{4} \left[\frac{g}{2\mu} (1 + 3\mu^2) \right]^{0.5} \rho D^{2.5} = j[(1 + 3\mu^2)/\mu]^{0.5} \quad (\text{Eq. 1})$$

where W is the flow rate, g is the gravitational acceleration, μ is the coefficient of internal friction, ρ is apparent density, and D is the diameter of the efflux tube.

One purpose of this study was to examine whether extrema in $\alpha = h(d)$ and $W = g(d)$ can logically produce extrema in $W = f(\alpha)$.

It is a general rule (9) in solid dosage form technology that a repose angle of 25–40° is a good working range. Therefore, for theory to fall in

Table I—Formulas for Granulations Used in the Repose Angle Studies

Ingredient	Granulation				
	I	II	III	IV	V
FD&C Yellow No. 5, g	6	—	—	—	—
Starch USP (dry), g	180	440	100	—	—
Lactose USP, g	1515	1755	1375	1000	1000
Starch USP (paste), g	45	15	—	—	—
Water, g	450	300	—	90	117
Sucrose USP, g	—	1110	—	—	—
Povidone, g	—	—	40	—	—
Alcohol USP (95%), g	—	—	360	—	—
Acacia, g	—	—	—	10	—
Gelatin, g	—	—	—	—	13

line with practice, Eq. 2 should yield a maximum in this repose angle range. Theoretical Eq. 2 is depicted in Fig. 1, and it is seen that the flow rate has a minimum (not a maximum) at $\mu = 0.6$. For a cohesionless powder:

$$\mu = \tan \alpha \quad (\text{Eq. 2})$$

so $\mu = 0.6$ corresponds to $\alpha = 30^\circ$. Kaneniwa *et al.* (17) classified powders of particle size below 50 μm as being cohesive, and Pilpel (16) classified powders in the 50–150- μm range as mildly cohesive; larger fractions are essentially noncohesive. These ranges are, of course, general rules and do not apply to all powders [carboxymethylcellulose and pyrogenic silica being notable exceptions (16)].

This study dealt with granulations of particle diameters above 150 μm . The intent was to show that repose angles of granulations essentially depend on the stacking characteristics, which explain the shallow maxima in α *versus* d curves.

EXPERIMENTAL

Five different formulations (Table I) were prepared. The dried granulations were screened through a nest of U.S. Standard sieves, and the various mesh fractions were subjected to angle of repose measurements in the following fashion. Bulk volume of material, 250 cc, was added to an aluminum funnel with the following dimensions: diameter at top, 10 cm; height from base of cone to apex, 7.5 cm; diameter of efflux tube, 0.95 cm; and height of efflux tube, 2.5 cm. The funnel was closed at the bottom of the efflux tube by fitting it flush with a piece of fiberboard, and the assembly was placed 10.2 cm (measured from the bottom of the efflux tube) above a piece of paper on a flat surface. The fiberboard was removed; the height, h , of the resulting heap was measured with a cathetometer; and the area of the base of the heap, A , was determined by cutting out the paper trace of the cone and weighing it (3). The repose

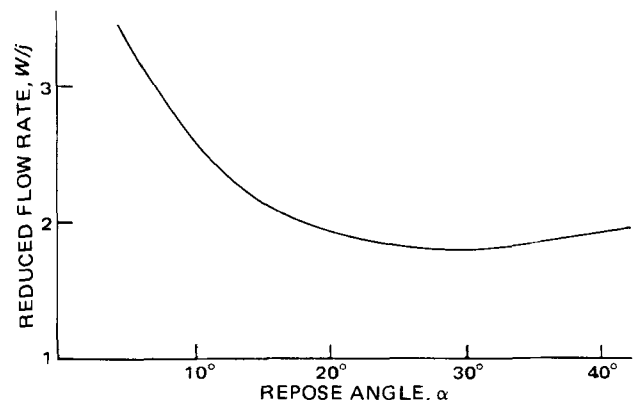


Figure 1— W/j as a function of $\alpha (= \tan^{-1} \mu)$ according to Eq. 1.

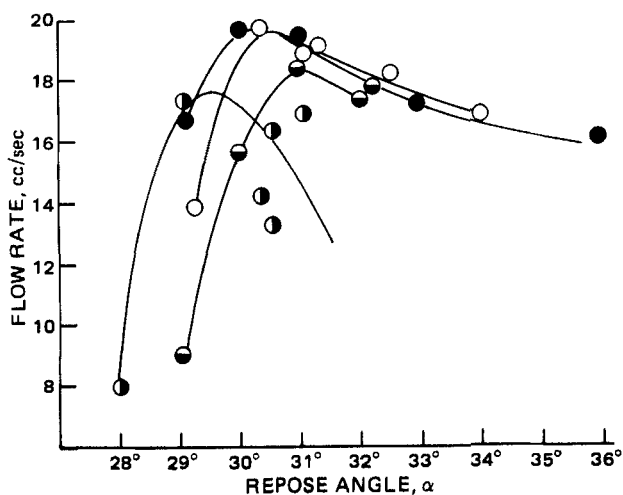


Figure 2—Flow rates as a function of repose angle based on a 100-g powder charge. Granulation V had relatively close α values (30.6–31.6) and could not be graphed in the scaling shown. Key: ○, Granulation I; ○, Granulation II; ○, Granulation III; and ●, Granulation IV.

angle, α , is then given by $\tan^{-1}[h/(\sqrt{A/\pi})]$. The flow rate was recorded by an electric timer.

Granulations I–III were tested again in a similar fashion using 100 g of each rather than 250 cc.

The porosities of the powder heaps were determined by determining the apparent densities of the heap and the particle density (not true density) of the granules. Since the height and the base area of the heap are known, the volume, v , can be calculated. The apparent density, ρ' , can then be calculated from the weight, L , as $\rho' = L/v$.

The particle densities were determined as follows. The procedure for determining true density pycnometrically using organic solvents was followed. The figure thus obtained was the volume of liquid displaced, V_1 , per sample weight, q_1 , of granules. Since some (but not total) solvent penetration can be expected, the particles were removed from the solvent and subjected to a drying curve. The point where the falling rate started was noted; the volume of solvent at this point corresponds to the volume of voids, V_2 , penetrated by the liquid. Hence, the particle density, ρ_p , is $q_1/(V_1 + V_2)$, and the bed porosity, ϵ_b , is then given by $\epsilon_b = 1 - (\rho'/\rho_p)$.

Povidone granulations could not be included in the part of the study dealing with α versus ϵ relationships, because of the solubility of povidone in organic solvents.

RESULTS AND DISCUSSION

Figure 1 shows that the flow of a particular granulation through a particular orifice should have a minimum for a granulation with an angle of repose of about 30°. Equation 1 predicts this finding because the de-

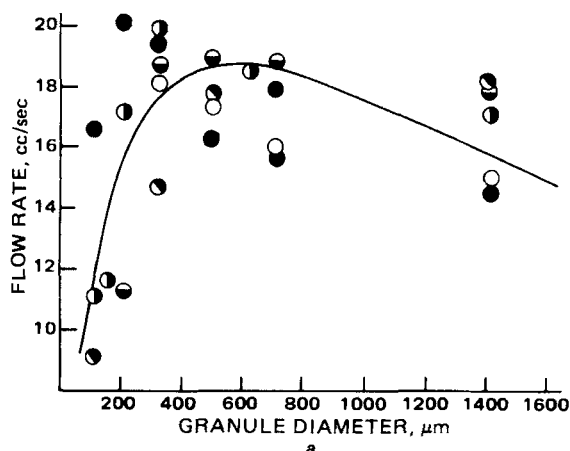


Table II—Repose Angles at which Flow Was Maximum

Granulation	Amount	Repose Angle at Maximum Flow	
		cc/sec	g/sec
I	250 cc	29.6°	29.6°
II	250 cc	29.4°	29.4°
III	250 cc	31.6°	29.8°
IV	220 cc	30.4°	29.2°
V	200 cc	30.8°	30.8°
I	100 g	30.7°	30.7°
II	100 g	29.3°	29.3°
III	100 g	31°	31°
IV	100 g	31°	30°
V	100 g	31.6°	30.6°

ivative with respect to μ of Eq. 1:

$$\frac{\partial W}{\partial \mu} = -0.5j[(1 + 3\mu^2)/\mu]^{-0.5}[3 - (1/\mu^2)] \quad (\text{Eq. 3})$$

equals zero when $\mu = \tan \alpha = 1/\sqrt{3}$ or when $\alpha = 30^\circ$. The second derivative of Eq. 3 is:

$$\frac{\partial^2 W}{\partial \mu^2} = -0.25j[(1 + 3\mu^2)/\mu]^{-1.5}[3 - (1/\mu^2)]^2 + 0.5j[(1 + 3\mu^2)/\mu]^{-0.5}(2/\mu^3) \quad (\text{Eq. 4})$$

This equation, when $\mu = 1/\sqrt{3}$ is inserted, gives the following value of the second derivative:

$$\frac{\partial^2 W}{\partial \mu^2} = -0 + 0.5j[(1 + 1)/\sqrt{3}]^{-0.5}2.3\sqrt{3} \quad (\text{Eq. 5})$$

which is larger than zero. Therefore, Eq. 1 does predict a *minimum* at a repose angle of 30° for a cohesionless powder. In contrast, the granulations reported here showed a *maximum* in flow rate at about 30–33° (Fig. 2 and Table II).

The different repose angles in this study were obtained by separating different mesh cuts of the granulations. Flow, of course, is a function of the mean diameter of the powder sample (10). The flow of the granulations is shown as a function of granule size in Fig. 3, and the flow exhibited the same dependence as reported elsewhere in the literature for powders (10) and granulations (19).

The repose angle, α , is plotted as a function of d , the mean mesh fraction diameter, in Fig. 4. A maximum occurred; this finding is somewhat different, functionally, from what has been reported in the literature for fine powders (4, 11) but is in accordance with some findings regarding coarse materials (16).

The behavior of granules is shown in Figs. 2–4; there are, of course, only two independent relations out of the three. The functional relations from Figs. 2, 3, and 4, respectively, are:

$$W = f(\alpha) \quad (\text{Eq. 6})$$

$$W = g(d) \quad (\text{Eq. 7})$$

and:

$$\alpha = h(d) \quad (\text{Eq. 8})$$

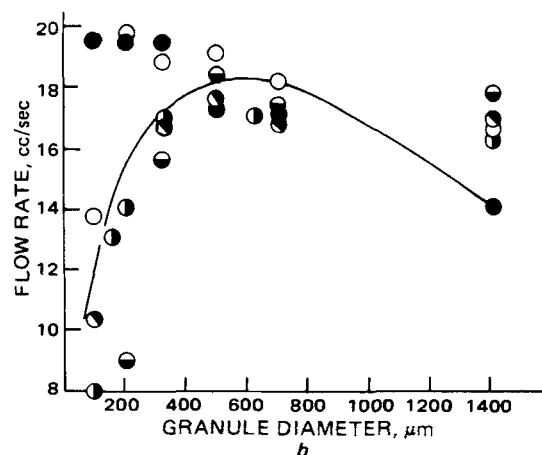


Figure 3—Flow rates as a function of granule diameter. Figure 3a is based on a 250-cc powder charge; Fig. 3b is based on a 100-g charge. Key: ○, Granulation I; ○, Granulation II; ○, Granulation III; ●, Granulation IV; and ○, Granulation V.

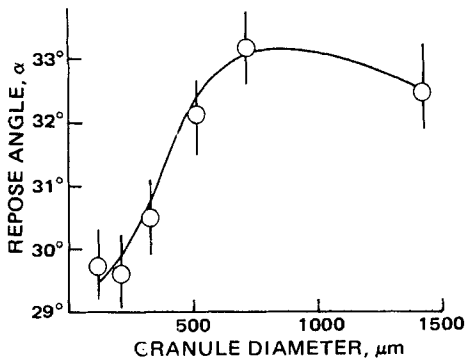


Figure 4—Repose angles as a function of particle diameter. Each point represents the average of the five granulations, and the bars indicate the 90% confidence limits on the average.

That a maximum can exist in all of the functional relationships is best demonstrated by approximating the curves in Figs. 2 and 4 by parabolas, *i.e.*:

$$W - W_{\max} = -k_1(\alpha - \alpha_{\max})^2 \quad (\text{Eq. 9})$$

and:

$$(\alpha - \alpha_{\max}) = -k_2(d - d_{\max})^2 \quad (\text{Eq. 10})$$

where the subscript max denotes the maximum value of the dependent variable or the value of the independent variable at which the dependent variable attains its maximum. The curves in Figs. 2 and 4 imply that extrema may occur but that they need not necessarily occur. One restriction in the argument given is that it assumes coinciding maxima in α and W .

If Eq. 10 is inserted in Eq. 9, then:

$$W - W_{\max} = -k_1k_2^2(d - d_{\max})^4 \quad (\text{Eq. 11})$$

which describes a curve with a maximum, *i.e.*, of the shape shown in Fig. 3.

A closely packed heap of spheres is shown in Fig. 5, and one (of many possible) metastable heap of loose packing is shown in Fig. 6. The porosity of a heap, as opposed to solid populations in confining vessels, has not been covered to any extent in the literature (18, 19). The apparent density of spheres in cylinders was discussed by Scott (20), who overcame difficulties stemming from wall effects (21) by plotting the packing density $(1 - \epsilon)$ versus the reciprocal of the vessel diameter $(1/D_0)$. He found a linear relationship, which, when extrapolated to $1/D_0 \rightarrow 0$ (*i.e.*, to $D_0 \rightarrow \infty$), gave a porosity of 0.36. This value compares favorably with the findings of Berg *et al.* (22) that one-dimensional vertical shaking of steel

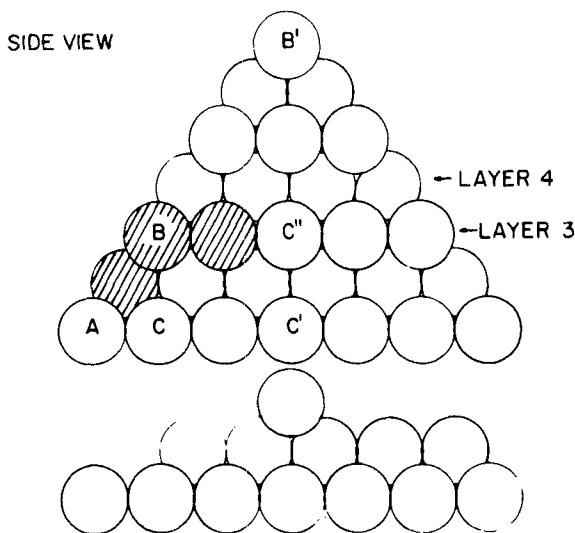


Figure 5—A closely packed heap of spheres. Key: top (AC'B'), unsupported by extra unloaded spheres; and left part of bottom (AC'C''), supported by an extra unloaded sphere (e.g., A) in each layer [*i.e.*, cross-hatched (B) spheres disappear].

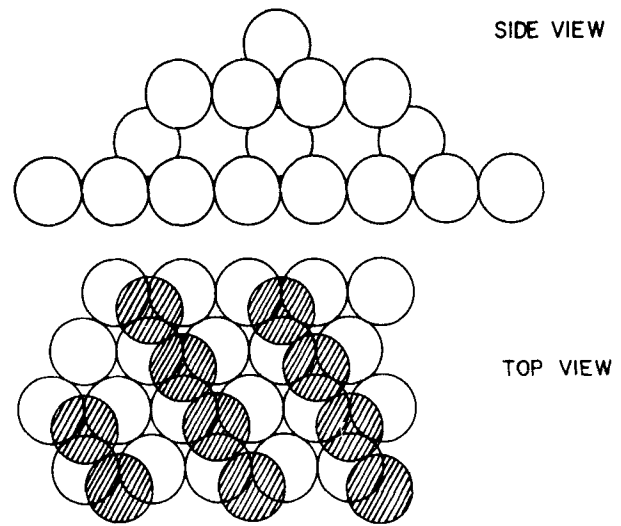


Figure 6—Loose packing resulting from removing every second sphere from every second layer in the supported structure shown in Fig. 5. The partially depleted layer is shown by cross-hatched spheres in an arbitrary layer.

spheres gave a porosity of 39% and that three-dimensional shaking gave 26% porosity and with the findings of Newitt and Conway-Jones (23) of a porosity of 38% for closely packed (wet) sand.

In each of these cases, the populations of steel balls or particles were confined by a vessel which, of course, makes them different from a heap. If a heap of spheres were cohesive, then loosely and closely packed heaps would have repose angles of the order of 60° as shown in Fig. 5. Indeed, Berg *et al.* (24) found a 60° angle of the powder remaining in a cubical container (where there is wall support). However, the 60° figure does not correlate with the finding here that the angles are in a range of $28\text{--}36^\circ$.

To evaluate the porosity of a conical heap, as shown in Fig. 5, circles were drawn as shown in Fig. 7 with radii $1.5d, 2.5d, \dots, qd/2$ about an arbitrarily chosen central sphere (S) in every second layer. For instance, as shown in Fig. 7, in layer 3 a circle with radius $2.5d$ is drawn around the central sphere and there are $q = 5$ spheres in the diagonal layer. In alternate layers, circles of radii $d, 2d, \dots, qd/2$ were drawn around the center of the diagonal which now is at the point (P) where two spheres touch. The number of spheres in a circle (layer) was counted with the arbitrary rule that if the center of a sphere were inside the circle, then the sphere was also "inside" the circle, *i.e.*, part of the layer.

For instance in Fig. 7, N and M are part of layer 4 but not part of layer 3. In this fashion it is possible to calculate the number of spheres in the top layer, the next highest layer, and so on; *i.e.*, the number of spheres can be calculated for successive values of q . The distance between each

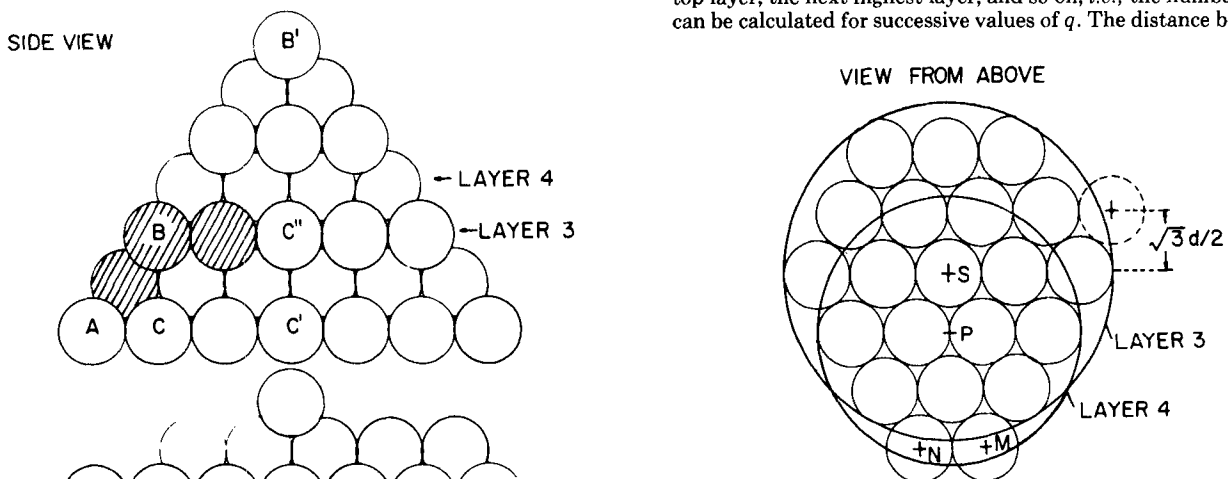


Figure 7—Spheres in two-dimensional close packing. In one layer, the center will be in the center of a sphere (S); in the layer above and below it, the center of the layer will be between two spheres (P). Spheres are counted as being inside the circle (part of the layer) if the center of a sphere is inside the circle. For instance, N and M are part of layer 4. The dotted sphere is not part of layer 3.

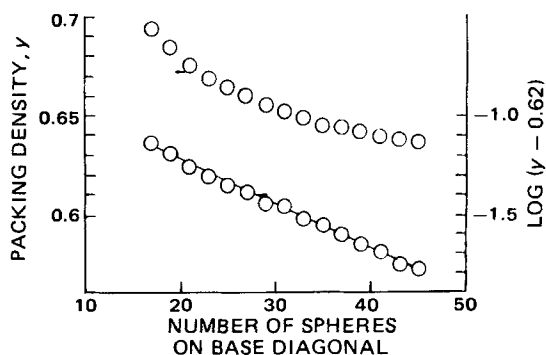


Figure 8—Packing densities of heaps as a function of the number of spheres on the diagonal of the base (number of layers in the heap) (upper curve). By assuming various asymptote values, subtracting these from the packing densities, and plotting them semilogarithmically versus q , the best straight line, i.e., the one with the smallest residual of squares (lower curve), occurred with an asymptote value of 0.62.

layer is $(\sqrt{2}/2)d$, so that the height of the cone is $[(q-1)(\sqrt{2}/2) + 1]d$, which approaches $q\sqrt{2}/2$ for large values of q . The area of the base is $\pi(dq)^2/4$; i.e., the cone volume can be calculated. Dividing the volume of all spheres by the cone volume then gives the packing density and, hence (by subtracting the latter from one), the porosity. Figure 8 shows that the packing density approaches 0.62 (i.e., $\epsilon = 0.38$). The bed porosities found in this study ranged from 0.28 to 0.54.

Making reference to Fig. 5 and noting that there are q spheres on the base diagonal, one sees that $AC' \rightarrow qd/2$ and $B'C' \rightarrow q\sqrt{2}d/2$ as $q \rightarrow \infty$. The repose angle hence approaches:

$$\alpha = \tan^{-1}\{qd\sqrt{2}/(qd)\} = 54.7^\circ \quad (\text{Eq. 12})$$

This value is obviously much higher than is generally encountered for cohesionless powders and granulations.

A conical heap (Fig. 5) is only stable if: (a) the friction between the plane support and the lower (outside) spheres is sufficiently high, and (b) the friction between spheres is sufficiently high to support the outside spheres. If this is not the case, the spheres "slip" out until there are sufficient spheres in the horizontal plane without spheres over them that can serve as retainers of the first sphere in the plane that carries spheres above it. If the cross-hatched spheres are removed, the shallower cone results, which has two supporting spheres on each diagonal. The diagonal of the base still contains q spheres, but the first layer above contains $q-3$ and the i th layer above the base contains $q-3i$ spheres on the diagonal. There would be $q/3$ layers in the center and the repose angle for large values of q would equal:

$$\alpha = \tan^{-1}\{(q/3)(\sqrt{2}/2)/(q/2)\} = \tan^{-1}(\sqrt{2}/3) = 25.2^\circ \quad (\text{Eq. 13})$$

With these assumptions and restrictions, it can be assessed that a closely packed conical heap has a repose angle of $\alpha_c = 25.2^\circ$ and a porosity of $\epsilon_c = 0.38$.

Loosely packed structures can be visualized in many ways. Figure 6 shows an example of a loose structure constructed by removing every second sphere in every second layer of the supported structure shown in Fig. 5. Therefore, the packing density would be $0.75 \times 0.62 = 0.46$; i.e., the porosity would be 0.54. The repose angle is obtained by noting that there are q (four) spheres to the right (and to the left) of the base center and that there are also q (four) layers (which are $d\sqrt{2}/2$ cm apart). Hence, the repose angle for large values of q approaches:

$$\alpha = \tan^{-1}\{(qd\sqrt{2}/2)/(qd)\} = \tan^{-1}(\sqrt{2}/2) = 35.3^\circ \quad (\text{Eq. 14})$$

The experimentally determined bed porosities ranged from 0.28 to 0.54, in agreement with the calculations, as is the fact that the repose angles ranged from 28.1 to 35.8°.

SUMMARY

1. For monodisperse granulations, experimental flow rates maximize (not minimize) at a particular repose angle around 30°.
2. Based on packing geometries and support layers, the expected repose angles should be 25.2–35.3°, which correlates well with experimental data ranging from 28.1 to 35.8°.
3. Based on packing geometries and support layers, the expected porosities should be 0.38–0.54; the experimentally determined bed porosities were in a range of 0.28–0.54.

REFERENCES

- (1) I. R. McDougall and A. C. Evans, *Rheol. Acta*, **4**, 218 (1965).
- (2) J. Gillard, L. Delattre, F. Jaminet, and M. Roland, *J. Pharm. Belg.*, **27**, 713 (1972).
- (3) D. Train, *J. Pharm. Pharmacol.*, **10**, 127T (1958).
- (4) N. Pilpel, *ibid.*, **16**, 705 (1964).
- (5) H. G. Kristensen and V. G. Jensen, *Dansk. Tidsskr. Farm.*, **43**, 104 (1969).
- (6) L. Delattre, J. Gillard, M. Roland, and F. Jaminet, *J. Pharm. Belg.*, **28**, 575 (1973).
- (7) F. A. Rocke, *Powder Technol.*, **4**, 180 (1970).
- (8) J. T. Carstensen, "Theory of Pharmaceutical Systems," vol. II, Academic, New York, N.Y., 1973, p. 187.
- (9) J. T. Carstensen, *ibid.*, p. 242.
- (10) R. Carr, *Chem. Eng.*, **67**(4), 121 (1960).
- (11) N. Kaneniwa, *Chem. Pharm. Bull.*, **15**, 1441 (1965).
- (12) G. Gold, R. N. Duvall, and B. T. Palermo, *J. Pharm. Sci.*, **55**, 1133 (1966).
- (13) G. Gold, R. N. Duvall, B. T. Palermo, and J. G. Slater, *ibid.*, **55**, 1291 (1966).
- (14) E. Hiestand, *ibid.*, **55**, 1325 (1966).
- (15) T. M. Jones and N. Pilpel, *J. Pharm. Pharmacol.*, **18**, 182S (1966).
- (16) N. Pilpel, "Advances in Pharmaceutical Science," vol. 3, Academic, New York, N.Y., 1971, p. 174.
- (17) N. Kaneniwa, A. Ikekawa, T. Ozaki, C. Shinya, N. Sugimoto, and Y. Hoxumi, *Yakugaku Zasshi*, **88**, 1642 (1968).
- (18) W. A. Gray, "The Packing of Solid Particles," Chapman & Hall, London, England, 1968, p. 125.
- (19) J. T. Carstensen, "Pharmaceutics of Solids," Badger Freund, Fond du Lac, Wis., 1974, p. 94.
- (20) G. D. Scott, *Nature*, **194**, 956 (1962).
- (21) *ibid.*, **188**, 909 (1960).
- (22) T. G. O. Berg, R. L. McDonald, and R. J. Trainor, Jr., *Powder Technol.*, **3**, 183 (1969).
- (23) D. M. Newitt and J. M. Conway-Jones, *Trans. Inst. Chem. Eng.*, **36**, 422 (1958).
- (24) T. G. O. Berg, R. L. McDonald, and R. J. Trainor, Jr., *Powder Technol.*, **3**, 56 (1969).

ACKNOWLEDGMENTS AND ADDRESSES

Received June 20, 1975, from the School of Pharmacy, University of Wisconsin, Madison, WI 53706.

Accepted for publication October 28, 1976.

* To whom inquiries should be directed.